

# Galactic Globular Cluster Metallicity Scale From the Ca II Triplet

## II. Rankings, Comparisons and Puzzles

Glen A. Rutledge, James E. Hesser, and Peter B. Stetson

National Research Council of Canada, Herzberg Institute of Astrophysics,  
Dominion Astrophysical Observatory, 5071 W. Saanich Rd., RR5, Victoria, BC V8X 4M6, Canada  
Electronic mail: firstname.lastname@hia.nrc.ca

### ABSTRACT

We compare our compilation of the  $W'$  calcium index for 71 Galactic globular clusters to the widely used Zinn and West (1984 ApJS, 55, 45)  $[\text{Fe}/\text{H}]$  scale and to Carretta and Gratton's (1997 A&AS, 121, 95) scale from high-dispersion spectra analyzed with Kurucz (1992, private communication) model atmospheres. We find our calcium ranking to be tightly correlated with each comparison set, in a non-linear and a linear fashion, respectively. By combining our calcium index information with the Zinn and West ranking, we are able to rank the globular clusters in our sample with a typical precision of  $\pm 0.05$  dex for  $[\text{Fe}/\text{H}]_{\text{ZW84}} \lesssim -0.5$ ; for clusters more metal rich than this, the ranking is less precise. The significant differences between these metallicity scales raise important questions about our understanding of Galactic formation and chemical enrichment processes. Furthermore, in spite of the apparent improvement in metallicity ranking for the Galactic globular clusters that results from our addition of information from the Ca II triplet lines to the potpourri of other metallicity indicators, caution – perhaps considerable – may be advisable when using  $W'$  as a surrogate for metallicity, especially for systems where ranges in age and metallicity are likely.

### 1. Introduction

In Paper I of this series (Rutledge et al. 1997), we presented new observations of the Ca II triplet lines at  $\lambda_{8498}$ ,  $\lambda_{8542}$ , and  $\lambda_{8662}$  in the spectra of 976 stars lying near the red giant branches (RGBs) of 52 Galactic globular clusters. The aim of this work is to establish a relative ranking of the clusters according to their calcium abundances, and to apply this ranking to some of the astrophysical problems associated with understanding the early stages of Galactic formation.

In §2, we summarize how the Ca II triplet is used to produce a calcium index,  $W'$ , for a given cluster, and how this index is related to the metallicity,  $[\text{Fe}/\text{H}]$ , of the cluster. A catalog of  $W'$  values for 71 clusters is created in §3 from a compilation of data from Paper I and from other studies. Zinn and West (1984, ZW84) produced a relative ranking of the globular clusters using a compilation of almost all the ranking techniques available at that time, to which we make

detailed comparisons in §4. Considering the past debate over the effect of HB morphology on Zinn’s (1980b) photometric  $Q_{39}$  index (Smith 1984, Frogel et al. 1983, ZW84), which plays a significant role in the  $[\text{Fe}/\text{H}]_{\text{ZW84}}$  scale, we have re-investigated this issue in §4.1 using our precise  $W'$  index and more recent HB types from Lee et al. (1994). We then make a detailed comparison of our calcium ranking with the  $[\text{Fe}/\text{H}]$  ranking of ZW84, which prove to be highly correlated, but in a *significantly non-linear* way. By combining the information in both systems, we are able to provide a metallicity ranking of improved precision (§4.3). In §5, we compare our calcium ranking to  $[\text{Fe}/\text{H}]$  values from high dispersion spectroscopy studies. We transform our calcium index to  $[\text{Fe}/\text{H}]$  on the Carretta and Gratton (1997, CG97) scale, which is highly correlated with our  $W'$  index in an *essentially linear* fashion. Finally, in §6, we briefly discuss the significance of these disparate metallicity scales and the use of the Ca II triplet lines as a metallicity indicator when studying Galactic formation physics.

## 2. Ca II Triplet as a Metallicity Indicator

The Ca II triplet lines at  $\lambda_{8498}$ ,  $\lambda_{8542}$ , and  $\lambda_{8662}$  are used to probe various astrophysical phenomena because they are among the strongest features in the near infrared spectra of most late-type stars and stellar systems, and thus their equivalent widths can be measured reasonably accurately for faint objects with moderate resolution spectrographs. Most of the early integrated light work took advantage of the sensitivity in the triplet’s summed equivalent width (denoted as  $\Sigma Ca$ ) to  $\log(g)$  as a means to discriminate between dwarf and giant populations (Spinrad and Taylor 1969, 1971, Anderson 1974). Initially, it was thought that  $\Sigma Ca$  was relatively insensitive to metallicity (Cohen 1978, 1979, Jones et al. 1984), but Alloin and Bica’s (1989) re-analysis of Jones et al.’s data found that metallicity does have a significant effect on  $\Sigma Ca$ . Diaz et al. (1989) found, from a sample of 106 bright stars with spectral classes F6-M0, that 97% of the variance in  $\Sigma Ca$  resulted from a linear combination of  $\log(g)$  and  $[\text{Fe}/\text{H}]$  with little dependence on  $T_{\text{eff}}$ . They suggested that  $[\text{Fe}/\text{H}]$  only plays a significant role when  $[\text{Fe}/\text{H}] \lesssim -0.3$  dex; otherwise,  $\log(g)$  is the dominant factor. The sensitivity of  $\Sigma Ca$  to  $[\text{Fe}/\text{H}]$  was not fully appreciated until it was measured for Galactic globular clusters and dwarf spheroidals.

Inspired by the success of the Ca II K line to rank globular clusters according to  $[\text{Fe}/\text{H}]$  (ZW84), Armandroff and Zinn (1988, AZ88) measured  $\Sigma Ca$  in the integrated light of 27 globular clusters and found very good correlations with other metallicity-sensitive indices. Since there is an intrinsic ambiguity in integrated light studies from the uncertainty in determining the fraction of light emitted by the various populations of stars, subsequent studies measured  $\Sigma Ca$  in individual RGB stars (Da Costa and Seitzer 1989, Olszewski et al. 1991, Suntzeff et al. 1992). A method of ranking globular clusters by  $[\text{Fe}/\text{H}]$  which is independent of both distance and reddening was devised by Armandroff and Da Costa (1991, hereafter AD91), and adopted by almost all later practitioners (Armandroff et al. 1992 [ADZ92], Da Costa et al. 1992 [DAN92], Suntzeff et al. 1993 [S93], Geisler et al. 1995 [G95], Da Costa and Armandroff 1995 [DA95], Suntzeff and Kraft 1996

[SK96], Paper I).

AD91 fully describe the technique, but we summarize the salient features. The  $\Sigma Ca$  is measured in probable member RGB stars as a function of the V magnitude above the horizontal branch (HB). Due to a combination of both  $\log(g)$  and  $T_{\text{eff}}$  decreasing as  $V_{HB} - V$  increases,  $\Sigma Ca$  increases going up the RGB with a slope of  $\sim 0.64 \text{ \AA mag}^{-1}$  (Paper I). It has been shown empirically that this slope is independent of the cluster metallicity (AD91, DA95, Paper I), and thus the  $\Sigma Ca$  of a red giant star in any cluster can be adjusted to the level of the HB by applying the correction  $\Sigma Ca_{HB} = \Sigma Ca - 0.64(V_{HB} - V)$ . The mean value of  $\Sigma Ca_{HB}$  for all RGB stars measured in the cluster is then denoted as the reduced equivalent width,  $W'$ , which is taken to be a calcium index for the entire cluster. For the 52 globular clusters we studied (Paper I), the  $W'$  values ranged from 1.58  $\text{\AA}$  for NGC 4590 ( $[\text{Fe}/\text{H}]_{ZW84} = -2.09$ ) to 5.41  $\text{\AA}$  for NGC 6528 ( $[\text{Fe}/\text{H}]_{ZW84} = +0.12$ ). With a typical  $\sigma(W')$  of  $\sim 0.08 \text{ \AA}$ , this provides approximately 48 resolution elements (each of  $\sim 0.05$  dex) with which to rank the globular clusters in  $[\text{Fe}/\text{H}]_{ZW84}$ .

### 3. Cluster Reduced Ca II Equivalent Widths: $W'$

A large number of  $\Sigma Ca$  measurements for globular cluster RGB stars are now found in the literature. We have transformed these to our Paper I system in two ways: the first involves transforming  $W'$  values, while the second involves transforming  $\Sigma Ca$  values and then calculating  $W'$  from them. As a result, 44 cluster  $W'$  values were transformed onto the Paper I system, 25 of which were in the Paper I sample. This increases the Paper I sample size from 52 to 71 clusters. The transformed  $W'$  values from the various authors, along with our final adopted  $W'$  value for each cluster, are presented in Table 1, where the columns are, respectively, 1) the consecutive cluster number; 2-4) the NGC, other cluster, and IAU names; 5) the  $W'$  values from Paper I; 6) the DA95  $W'$  values transformed to the Paper I system, as described by the first method below; 7) other  $W'$  values transformed to the Paper I system, as described by the second method below; 8) the final adopted  $W'$  value calculated as described below; and 9) the reference from which the  $\Sigma Ca$  values were taken to calculate the  $W'$  given in column 7. The number following the  $\pm$  sign in columns five through eight represent our one sigma error estimates on these values.

DA95 transformed the  $\Sigma Ca$  values of AD91, DAN92, ADZ92, and S93 onto their system to calculate  $W'$  values for their calibrating globular clusters. Using 13 globular clusters that we observed in common with DA95, we obtain the linear regression (see Figure 1),

$$W'_{\text{Paper I}} = 0.94(\pm 0.02) \cdot W'_{\text{DA95}} + 0.06(\pm 0.02) \quad m.e.1 = 1.35,$$

using an algorithm which allows for errors in both directions (Stetson 1989). As described in Paper I, the *m.e.1* value is a  $\chi^2$  variable which measures the scatter about the fit, where a value of one indicates that the scatter is consistent with the observational errors, and larger values indicate that either the errors have been underestimated or the relation is non-linear. The above regression was used to transform 24  $W'$  values from DA95 onto our Paper I system (see Table 1),

where the errors tabulated include transformation errors. We did not use NGC 5927 to determine the regression due to the problems discussed by DA95<sup>1</sup>.

For the remainder of the clusters in AD91, ADZ92, DAN92 and S93 that DA95 did not use as calibrating clusters, and for the clusters observed by G95 and SK96, the following transformation technique was used. The individual  $\Sigma Ca$  values were transformed onto the Paper I system using the regressions given in Table 6 of Paper I, where the errors attached to each value include the errors incurred from the transformation. The  $W'$  of each cluster was then calculated as the weighted mean of  $\Sigma Ca - 0.64(V_{HB} - V)$  for each star in the cluster, where the weights were assigned as  $1/\sigma^2$ . The errors for these  $W'$  values, listed in column 7 of Table 1, were calculated as  $(\Sigma 1/(\sigma^2))^{-0.5}$  if the *m.e.1* value was  $\leq 1.0$ , and as *m.e.1*  $\cdot (\Sigma 1/(\sigma^2))^{-0.5}$  if *m.e.1* was  $> 1.0$ , where the sum is taken over the number of stars observed in the cluster. In total, 21 cluster  $W'$  values were transformed onto the Paper I system using this technique.

The adopted  $W'$  value for each cluster was calculated as a weighted mean of the individual  $W'$  values listed in Table 1, where the weights were assigned as  $1/\sigma^2$ . The errors were calculated as  $(\Sigma 1/(\sigma^2))^{-0.5}$  if the *m.e.1* value was  $\leq 1.0$ , and as *m.e.1*  $\cdot (\Sigma 1/(\sigma^2))^{-0.5}$  if *m.e.1* was  $> 1.0$ , where the sum is taken over the available  $W'$  values discussed above. In order to calculate the  $W'$  index, it is necessary to measure the V magnitude of the HB, which introduces another source of error in  $W'$ . We have allowed for an uncertainty of  $\pm 0.1$  mag in  $V_{HB}$ , by adding in quadrature an additional error of  $\pm 0.064 \text{ \AA}$  to the error estimate described above. This final error estimate is given in column 8 of Table 1.

#### 4. The Zinn and West Relative Metallicity Scale

The relative metallicities of globular clusters can be estimated by a variety of techniques (Kraft 1979), most of which measure either line blocking in the cluster integrated light, or some metallicity sensitive parameter in the color-magnitude diagram (CMD), while some of the more recent techniques employ equivalent width measurements of strong spectral features. The ZW84 [Fe/H] scale is a relative ranking of 121 Galactic globular clusters placed on Cohen’s (see Frogel et al. 1983 for a compilation and references) metallicity scale with a precision of  $\sim 0.1$  dex. ZW84

---

<sup>1</sup>Of the 14 NGC 5927 stars discussed by DA95, three were contaminated by TiO, six had  $\Sigma Ca$  values close to the 47 Tuc fiducial, and five had  $\Sigma Ca$  values  $\sim 0.6 \text{ \AA}$  larger. They used the five larger values to define  $W'$  for NGC 5927, and proposed that the bifurcation is most likely a result of rather large errors in the photometry they used (Menzies 1974) and/or differential reddening across the cluster, as suggested by Menzies and more recently by Cohen and Sleeper (1995). Unfortunately, the stars in our Paper I sample were not observed in the new CCD photometry of NGC 5927 (Sarajedini and Norris 1994), so we could not test DA95’s hypothesis. Since the scatter of the 11 stars about our fit to this cluster is consistent with our observational errors, it seems that differential reddening among our stars was not appreciable. (The stars from DA95 and Paper I were both selected to avoid the region defined by Menzies (1974) to be differentially reddened.) Our final  $W'$  value for this cluster is simply the weighted mean of the transformed DA95 value and the Paper I value.

combined a variety of relative ranking indices to increase their sample size and average over various observational uncertainties. Since the ZW84 scale has been widely applied and contains the information present in most relative ranking indices available at the time of its compilation, we first focus our attention on it.

#### 4.1. $Q_{39}$ Ranking

Seventy-nine globular clusters were ranked with the photometric  $Q_{39}$  index (Zinn 1980b), which is a filter system applied to integrated light to measure line blocking over  $\sim 190 \text{ \AA}$  centered on the Ca II H and K lines. Integrated light spectrograms of 60 clusters were subsequently used to measure the pseudo-equivalent widths of the Ca II K, the G band, and the Mg I  $b$  lines (ZW84). These rankings were transformed to  $Q_{39}$  values, which increased the number of clusters with observed or inferred  $Q_{39}$  indices to 74. The weighted mean of  $Q_{39}$  was taken by ZW84 to determine the spectroscopically augmented  $Q_{39}$  values for clusters with more than one estimate. Except where specifically noted, we adopt the spectroscopically augmented  $Q_{39}$  values of ZW84 for use throughout this paper; were the photometric  $Q_{39}$  values used in the final analysis, our results would not change significantly. Due to higher  $T_{\text{eff}}$  values, blue HB stars produce great flux at ultraviolet wavelengths. Therefore, clusters with extremely blue HBs are expected to have their  $Q_{39}$  values diluted by this flux, and thus their  $[\text{Fe}/\text{H}]$  values underestimated. For the photometric  $Q_{39}$  index, Manduca (1983) provides theoretical support for this effect, while Smith (1984) and Frogel et al. (1983) provide observational evidence. However, ZW84 provide counter arguments which suggest that their spectroscopically augmented  $Q_{39}$  is only weakly dependent on HB morphology, if at all.

In Figure 2, we plot each of these four  $Q_{39}$  indices against  $W'$ , where symbols represent different ranges in  $(B - R)/(B + V + R)$  (Lee et al. 1994). The  $Q_{39}$  values employed in the bottom right panel of Figure 2 are the purely photometrically determined  $Q_{39}$  indices. All four indices correlate well but non-linearly with  $W'$ ; indeed, all suggest a break at  $W' \sim 3.5\text{-}4.0$ . In the present sample, the second-parameter problem appears in its full-blown form over a surprisingly narrow range of calcium-triplet strength: the calcium-weakest cluster with a predominantly red HB [ $(B - R)/(B + V + R) < 0$ ] is NGC 362, with  $W' = 3.72 \text{ \AA}$ , while the calcium-strongest cluster with a predominantly blue HB [ $(B - R)/(B + V + R) > 0$ ] is NGC 6266, with  $W' = 4.01 \text{ \AA}$ . This range of  $W'$  corresponds approximately to  $-1.40 \leq [\text{Fe}/\text{H}]_{\text{ZW84}} \leq -1.25$ . This is in contrast to some earlier studies<sup>2</sup>, e.g. Lee, Demarque, and Zinn (1994), which found the second-parameter effect to extend over the range  $-2.0 \lesssim [\text{Fe}/\text{H}] \lesssim -1.1$ . Therefore, the possibility exists that previous

---

<sup>2</sup> However, note that the present sample does not include the northern clusters M3 = NGC 5272 and NGC 7006, which form a famous second-parameter trend with M13 = NGC 6205 and M2 = NGC 7089 at a metallicity near  $[\text{Fe}/\text{H}] = -1.6$  on this scale. Still, even M3 has a “bluish” HB in the sense of the present discussion, with  $(B - R)/(B + V + R) = 0.08$ .

estimates of the *extent* of the second-parameter problem may have been inflated slightly by the inclusion of clusters with metallicities as uncertain as  $\pm 0.2$  or  $\pm 0.3$  dex. Only the accumulation of a considerably larger sample of highly precise metallicity indicators will delimit the true abundance range of the second parameter effect. However, within the restricted range  $-1.40 \lesssim [\text{Fe}/\text{H}]_{\text{ZW84}} \lesssim -1.25$  it is certainly true that the second parameter problem is real, as clusters of all five HB classes are found there: our “very blue”, “blueish,” “reddish,” and “very red” classes, as well as the prototype of the “bimodal HB” class, NGC 2808. Within the narrow range  $3.72 \text{ \AA} \leq W' \leq 4.01 \text{ \AA}$ , it is evident from the bottom right panel of Figure 2 that (within the small-number statistics of the present sample) clusters with red HBs (closed symbols) tend to have larger values of the photometric  $Q_{39}$  index than those with blue HBs (open symbols) of comparable  $W'$  values. Furthermore, if we extend the range under consideration to  $3.3 \text{ \AA} \lesssim W' \lesssim 4.3 \text{ \AA}$ , it appears that clusters with blueish HBs (open diamonds) tend to lie above those with very blue HBs (open triangles) and clusters with very red HBs (closed circles) tend to lie above those with reddish HBs (closed squares). Thus, the photometric  $Q_{39}$  index appears to increase systematically from clusters with very blue, to blueish, to reddish, to very red HBs at  $[\text{Fe}/\text{H}]_{\text{ZW84}} \sim -1.3$ . Given the present sample size, this result is hardly definitive, but it does provide (weak) support to the contention of Manduca (1983), Smith (1984), and Frogel et al. (1983), that the photometric  $Q_{39}$  index is affected by differences in HB morphology at fixed metal abundance. However, little or no corresponding trend of Ca II K-line strength, Mg I b strength, or G-band strength with HB morphology is seen (the other three panels of Figure 2). A more detailed discussion of the implications of these observations is given in the next section.

#### 4.2. Horizontal-Branch Morphology and $[\text{Fe}/\text{H}]_{Q_{39}}$

The relative ranking of the majority of the globular clusters in ZW84 has been determined either from 1) the  $Q_{39}$  index,  $[\text{Fe}/\text{H}]_{Q_{39}}$ , or, 2) the weighted mean of eight other independent ranking indices,  $[\text{Fe}/\text{H}]_{\text{avg}}$ , or 3) the average of the two. We have plotted the  $[\text{Fe}/\text{H}]$  derived from each of the first two methods, as well as the difference between them (if both measures are available), as a function of  $W'$  in Figure 3. Both  $[\text{Fe}/\text{H}]$  values show very good correlation with  $W'$ , but again, both are obviously non-linear with respect to  $W'$ . The mean difference ( $[\text{Fe}/\text{H}]_{Q_{39}} - [\text{Fe}/\text{H}]_{\text{avg}}$ ) for all clusters in common is  $-0.018 \pm 0.17 \text{ \AA}$ . This scatter is roughly consistent with the expected observational errors, as noted by ZW84, but there are a few features in the bottom panel that should be emphasized.

At the metal-poor end, the  $[\text{Fe}/\text{H}]$  values are in good agreement except for NGC 6397, for which  $[\text{Fe}/\text{H}]_{Q_{39}}$  is  $\sim 0.4$  dex lower than  $[\text{Fe}/\text{H}]_{\text{avg}}$ . At the metal rich end,  $[\text{Fe}/\text{H}]_{Q_{39}}$  is slightly larger than  $[\text{Fe}/\text{H}]_{\text{avg}}$  for every cluster except NGC 6352, which only has a spectroscopic  $Q_{39}$  value. Excluding this cluster, the mean value of  $\Delta[\text{Fe}/\text{H}]$  for the five clusters with  $W' > 4.5 \text{ \AA}$ , and  $(B - R)/(B + V + R) \leq -0.5$  (*i.e.* very red HBs) is  $0.13 \pm 0.02$  (*s.d.m.*) dex. In the range of  $W'$  from 2.5 to 4.5  $\text{ \AA}$ , all of the clusters with  $(B - R)/(B + V + R) > 0.5$  (*i.e.* very blue HBs)

have  $\Delta[\text{Fe}/\text{H}]$  values less than zero, except NGC 5286, and NGC 6218<sup>3</sup>. Similarly, all clusters in this range with  $(B - R)/(B + V + R) \leq -0.5$  have  $\Delta[\text{Fe}/\text{H}]$  values greater than zero, except NGC 6712.

From the studies of §4.1 and this section, we conclude that HB morphology does influence the  $Q_{39}$  index, but, given the latter’s significant observational uncertainties, HB morphology likely has little influence on the overall  $[\text{Fe}/\text{H}]_{ZW84}$  ranking. Accordingly, we have combined the ZW84  $[\text{Fe}/\text{H}]$  ranking with our  $W'$  ranking to produce a relative metallicity scale of (presumably) greater precision for the globular clusters in our sample.

### 4.3. Most Probable cluster abundance on the Zinn and West Scale - $\langle [\text{Fe}/\text{H}]_{ZW84} \rangle$

The ZW84  $[\text{Fe}/\text{H}]$  values are plotted against  $W'$  in Figure 4, where the symbols represent the different techniques used to calculate  $[\text{Fe}/\text{H}]_{ZW84}$ . In the upper panel, we plot those clusters which have  $[\text{Fe}/\text{H}]_{ZW84}$  values which were calculated as the weighted mean of  $[\text{Fe}/\text{H}]_{Q39}$  and  $[\text{Fe}/\text{H}]_{avg}$ . This mean should reduce the sensitivity of  $[\text{Fe}/\text{H}]_{ZW84}$  to HB morphology, as well as represent a well defined set of  $[\text{Fe}/\text{H}]$  values. We fit a cubic polynomial allowing for errors in both directions,

$$[\text{Fe}/\text{H}]_{ZW84} = -3.005 + 0.941W' - 0.312W'^2 + 0.0478W'^3 \quad m.e.1 = 0.59,$$

which allows  $[\text{Fe}/\text{H}]_{ZW84}$  and  $W'$  metallicity rankings to be merged onto a common system.

NGC 1851 was not used in the regression due to its sensitive, and seemingly anomolous position, near the upturn of the fit<sup>4</sup>. The exclusion of any other cluster from the regression (including NGC 5927 and NGC 6218) does not significantly affect the fit. Previous practitioners have generally calibrated their  $W'$  index to the ZW84 scale using two straight lines with a break at  $W' \sim 3.75 \text{ \AA}$  (DA95, SK96). We have transformed the calibration lines of DA95 to the Paper I system and overplotted them on our data in Figure 4. For  $W' \lesssim 4.75 \text{ \AA}$ , the maximum deviation of our cubic fit from these calibration lines is  $\sim 0.05$  dex. However, for  $W' > 4.75 \text{ \AA}$ , the deviations become much larger, which no doubt reflects uncertainties in both quantities for the metal-richer clusters. The excellent agreement between our cubic polynomial and DA95’s two linear relations for clusters having  $W' < 4.75 \text{ \AA}$  suggests both that we have adequately transformed DA95  $W'$  values onto our system, and that the final calibration with  $[\text{Fe}/\text{H}]_{ZW84}$  by either approach is indistinguishable within the observational uncertainties.

In the bottom panel, all the clusters in our sample with  $[\text{Fe}/\text{H}]_{ZW84}$  values are plotted. It is apparent that much of the scatter in this relation is caused by  $[\text{Fe}/\text{H}]_{ZW84}$  values that were not

---

<sup>3</sup> The clusters NGC 6266 and NGC 6626, which were used to analyze the dependence of the photometric  $Q_{39}$  on HB type in §4.1, are not present in this plot since they do not have  $[\text{Fe}/\text{H}]_{avg}$  values.

<sup>4</sup> NGC 1851’s anomolous position was also noted by AD91 in their Figure 4.

derived from the weighted mean of  $[\text{Fe}/\text{H}]_{Q39}$  and  $[\text{Fe}/\text{H}]_{avg}$ , which indicates that the predominant source of the scatter is in  $[\text{Fe}/\text{H}]_{ZW84}$ . In order to incorporate the information present in both scales, we have determined the most probable position of each cluster on the cubic polynomial. This is done by calculating the point on the polynomial curve that penetrates most deeply into the nest of error ellipses centered on the observed position of each cluster (Stetson 1989). The results of this procedure are presented in Table 2, where the columns are respectively: 1,2) NGC and other names; 3)  $[\text{Fe}/\text{H}]_{ZW84}$  as given by ZW84, with updates taken from Zinn (1985); 4,5)  $\langle W' \rangle, \langle [\text{Fe}/\text{H}]_{ZW84} \rangle$ , which are the most probable values of these quantities calculated as described above; 6)  $[\text{Fe}/\text{H}]_{CG97}$ , which are the  $[\text{Fe}/\text{H}]$  values derived from transforming our  $\langle W' \rangle$  onto the high dispersion  $[\text{Fe}/\text{H}]$  scale of CG97 (see §5); and 7) notes for individual clusters.

The numbers after the  $\pm$  sign in columns 4-6 represent our  $1\sigma$  error estimates on these quantities. The error estimates for  $[\text{Fe}/\text{H}]_{CG97}$  are described in §5, while the error estimates for  $\langle W' \rangle$  and  $\langle [\text{Fe}/\text{H}]_{ZW84} \rangle$  were calculated as follows:

$$\begin{aligned} \sigma_{\langle [\text{Fe}/\text{H}]_{ZW84} \rangle} &= K \cdot \left( \frac{1}{\sigma_{[\text{Fe}/\text{H}]_{ZW84}}^2} + \frac{1}{m^2 \cdot \sigma_{W'}^2} \right)^{-0.5}, \\ \sigma_{\langle W' \rangle} &= K \cdot \left( \frac{1}{m^{-2} \cdot \sigma_{[\text{Fe}/\text{H}]_{ZW84}}^2} + \frac{1}{\sigma_{W'}^2} \right)^{-0.5}, \end{aligned}$$

where  $\sigma_{[\text{Fe}/\text{H}]_{ZW84}}$  is listed in column 3 of Table 2,  $\sigma_{W'}$  is listed in column 8 of Table 1,  $m$  is the gradient of the cubic polynomial at  $\langle W' \rangle$  in units of  $\text{dex } \text{\AA}^{-1}$ , and  $K$  is the ratio of the deviation from the fit,  $((W' - \langle W' \rangle)^2 + ([\text{Fe}/\text{H}]_{ZW84} - \langle [\text{Fe}/\text{H}]_{ZW84} \rangle)^2)^{0.5}$ , to the expected  $1\sigma$  deviation,  $(\sigma_{[\text{Fe}/\text{H}]_{ZW84}}^2 + \sigma_{W'}^2)^{0.5}$ .  $K$  is restricted to be  $\geq 1$ . The typical precision with which these clusters can now be ranked on the ZW84 scale is  $\sim \pm 0.05$  dex, which is an improvement over the original ZW84 precision by a factor of  $\sim 2$ . It should be emphasized that the  $\sigma$  values attached to these quantities represent the precision with which the clusters can be ranked, and not the accuracies. The absolute metallicity scale is uncertain by at least 0.2 dex, as discussed in §5.

The metal-rich portion of the transformation is made uncertain by the lack of high quality data. The cubic polynomial that we have employed, and the linear fit employed by DA95 diverge significantly in this region, but the most probable positions of the clusters do not change drastically depending on what calibration line is used. For example, NGC 5927 has a most probable value on the cubic polynomial of  $-0.32 \pm 0.08$  dex, whereas on the DA95 line, it has a most probable value  $\sim -0.42$  dex. The most probable value of NGC 6553 is  $-0.18 \pm 0.12$  dex on the cubic fit, and  $\sim -0.29$  dex on the DA95 line. NGC 6528, which is not listed in Table 2 since it lies beyond the last calibrating cluster, has a most probable value on the cubic polynomial of  $+0.28 \pm 0.16$  dex, whereas on the DA95 line, it has a most probable value  $\sim 0.0$  dex. Therefore, even though



the calibration of the  $[\text{Fe}/\text{H}]_{\text{ZW84}}$  values for the metal-rich clusters is uncertain, relative rankings appear to be robust.

## 5. High Dispersion Metallicity Scales

Ultimately, the absolute  $[\text{Fe}/\text{H}]$  scale must be established through curve-of-growth analysis of high dispersion spectra (henceforth referred to as HDS) for many globular cluster stars. However, due to the susceptibility of such analysis to systematic errors, which escalate rapidly as  $[\text{Fe}/\text{H}]$  increases, the absolute  $[\text{Fe}/\text{H}]$  scale is still the subject of considerable controversy (CG97). The debate over the metal-rich end of the metallicity scale in the early 1980’s is well known (see, e.g., Freeman and Norris 1981), where photographic HDS with echelle spectrographs (Pilachowski et al. 1980, Cohen 1980) yielded significantly smaller  $[\text{Fe}/\text{H}]$  values than previously suspected. For this reason, the ZW84 scale is not based entirely on high-dispersion results, as discussed in §6.1.

In an attempt to provide a modern high-dispersion calibration for our  $W'$  index, we have culled from the literature all the recent HDS  $[\text{Fe}/\text{H}]$  estimates from groups who have studied at least four of the clusters in our sample. These values are presented in Table 3 where the columns are, respectively: 1,2) NGC and other names; 3)  $[\text{Fe}/\text{H}]$  values of Cohen used to calibrate the ZW84 scale; and 4-8) the  $[\text{Fe}/\text{H}]$  values of five different HDS groups; the references for each group are listed at the bottom of the table. For a given cluster, the range of  $[\text{Fe}/\text{H}]$  values from different groups indicates that the absolute metallicity scale is still uncertain by at least 0.2 dex.

We compare our calcium  $W'$  index to the  $[\text{Fe}/\text{H}]$  values determined by individual groups<sup>5</sup> in Figure 5, where the solid line overplotted on the data is the cubic polynomial fit to the  $[\text{Fe}/\text{H}]_{\text{ZW84}}$  data. The  $[\text{Fe}/\text{H}]$  values of Cohen show the same non-linear relationship to  $W'$  as  $[\text{Fe}/\text{H}]_{\text{ZW84}}$ , since the ZW84 scale was calibrated with her data. However, none of the other HDS  $[\text{Fe}/\text{H}]$  results show any strong evidence for a non-linear relationship with  $W'$ . This corroborates the suggestion of CG97 that the ZW84  $[\text{Fe}/\text{H}]$  scale may be non-linear with respect to the true  $[\text{Fe}/\text{H}]$  scale.

The  $[\text{Fe}/\text{H}]$  scale defined by CG97 is based upon the largest, most self-consistent HDS analysis that presently exists for the globular clusters. They have reanalyzed high quality equivalent widths from several different sources, including GO89, M93, and SKPL, using a homogeneous compilation of stellar atmosphere parameters,  $gf$  values, and the Kurucz (1992) stellar atmospheres. A linear fit which allows for errors in both directions yields,

$$[\text{Fe}/\text{H}]_{\text{CG97}} = -2.66(\pm 0.08) + 0.42(\pm 0.02) \cdot \langle W' \rangle \quad m.e.1 = 1.51.$$

This relation is plotted as a dotted line in Figure 5, and is used to transform the  $\langle W' \rangle$  values

---

<sup>5</sup> We assume that analyses done within a given group make the same assumptions about  $gf$  values, the absolute solar Fe abundance,  $T_{\text{eff}}$  scale, etc.

into  $[\text{Fe}/\text{H}]_{CG97}$  in Table 2. The errors have simply been calculated as,

$$\sigma_{[\text{Fe}/\text{H}]_{CG97}} = m \cdot \sigma_{\langle W' \rangle},$$

where  $m$  is the slope of the above linear relation in units of  $\text{dex } \text{\AA}^{-1}$ , and  $\sigma_{\langle W' \rangle}$  is listed in Table 2. We have not included the transformation errors since we are only interested in how the clusters rank on this scale. As stated in §4.3,  $\sigma_{[\text{Fe}/\text{H}]_{CG97}}$  represents the precision with which the cluster can be ranked, and not the accuracy. For the calcium index, we chose to use the most probable value,  $\langle W' \rangle$ , rather than the measured value,  $W'$ , since the technique used in §4.3 to calculate  $\langle W' \rangle$  adds information from the various ranking systems upon which the ZW84 scale is based and, thus, is likely to improve the precision of relative ranking. However, for any cluster whose  $[\text{Fe}/\text{H}]_{CG97}$  value changes by more than 0.05 dex when  $W'$  is used in the calibration instead of  $\langle W' \rangle$ , we list what  $[\text{Fe}/\text{H}]_{CG97}$  would be in a footnote to Table 2.

## 6. Discussion

The foregoing determination of globular cluster  $W'$  indices appears to have increased by a factor of  $\sim 2$  the precision with which we can rank globular clusters by metallicity on a scale based upon  $[\text{Fe}/\text{H}]_{ZW84}$ . Such an improvement would appear to support the effectiveness of the Ca II triplet as a metallicity indicator, especially in the context of AD91’s  $W'$  index for old, metal-poor stellar systems. In spite of our apparent success, we feel rather sobered by issues surrounding the metallicity scale and the widespread use of the Ca II triplet as a surrogate for overall metal abundance, as we briefly discuss here.

### 6.1. $W'$ and Other Scales

As shown above,  $W'$  is tightly correlated with  $[\text{Fe}/\text{H}]$  for the globular clusters we have studied. Disturbingly, however, a significantly non-linear correlation with  $[\text{Fe}/\text{H}]_{ZW84}$  contrasts sharply with the linear correlation we find with  $[\text{Fe}/\text{H}]_{CG97}$ . We have no particular *a priori* reason to expect how  $W'$ , an empirical line-strength measure, should be related to  $[\text{Fe}/\text{H}]$ , and it is unclear which, if either,  $[\text{Fe}/\text{H}]$  scale to trust.

The sense of the non-linear relation between  $W'$  and  $[\text{Fe}/\text{H}]_{ZW84}$  is that the abundance sensitivity of  $W'$  decreases as the abundance on the  $[\text{Fe}/\text{H}]_{ZW84}$  scale increases (AD91, DAN92, S93, DA95, SK96). Most of the preceding authors chose to transform their  $W'$  values into  $[\text{Fe}/\text{H}]_{ZW84}$  via two linear relations with a break at  $[\text{Fe}/\text{H}]_{ZW84} \sim -1.5$ . Three potential reasons for the decrease in abundance sensitivity of  $W'$  with increasing abundance were outlined by AD91, but to our knowledge this issue has not been significantly explored since. AD91 proposed that: i) weak metal lines and molecular bands of TiO may be depressing the pseudo-continuum in the more metal-rich clusters, thereby resulting in smaller measured  $\Sigma Ca$  values; ii) at higher

abundances, the increase in the strength of the Ca II lines occurs mostly in the wings, where it is harder to measure than in the line cores<sup>6</sup>; and finally, iii) [Ca/Fe] actually does decrease with increasing [Fe/H].

There are at least two other effects that should be considered when trying to understand this nonlinearity. Firstly, as noted by AZ88,  $W'$  increases with [Fe/H] both because the abundance of Ca in the atmosphere is larger, and because  $\log(g)$  at the level of the HB is smaller. Furthermore, an increase in cluster [Fe/H] causes  $T_{\text{eff}}$  at the level of the HB to be smaller. Despite the earlier studies, Jorgensen et al. (1992) have shown through synthetic spectra calculations that  $\Sigma Ca$  has a relatively large and complex dependence on  $T_{\text{eff}}$  in the globular cluster metallicity range. It is clear that  $W'$  is sensitive to more than just a simple abundance increase in globular clusters as their RGBs shift in the  $\log(g)$ ,  $T_{\text{eff}}$  plane.

Secondly,  $W'$  may appear to lose sensitivity to [Fe/H] for the higher metallicity clusters because all comparisons, so far, have been made between  $W'$  and  $[\text{Fe}/\text{H}]_{ZW84}$ , which may itself be non-linear with respect to the true [Fe/H] (CG97 and below). The relative indices used by ZW84 were placed on the [Fe/H] scale compiled by Frogel et al. (1983). For  $[\text{Fe}/\text{H}] \leq -1.5$ , the scale is based on the early high-dispersion photographic spectroscopy of individual giant stars by Cohen (1978b, 1979b, 1981) and Cohen and Frogel (1982), while for the more metal-rich clusters, it is based on models of line blocking in low-dispersion scans of individual stars (Cohen 1982, 1983). It is interesting that the “break” in linearity between  $W'$  and  $[\text{Fe}/\text{H}]_{ZW84}$  also occurs at  $[\text{Fe}/\text{H}]_{ZW84} \sim -1.5$ . In addition, if only clusters with  $[\text{Fe}/\text{H}]_{ZW84} \lesssim -1.5$  are used to compare  $[\text{Fe}/\text{H}]_{ZW84}$  and  $[\text{Fe}/\text{H}]_{CG97}$ , there is very little evidence for a non-linear relationship between them.

In summary, possible reasons for the non-linear relationship between  $W'$  and  $[\text{Fe}/\text{H}]_{ZW84}$  can be split into three classes: i) it is a result of how  $\log(g)$  and  $T_{\text{eff}}$  (and possibly turbulent velocity) of the RGB stars vary for clusters of different [Fe/H] and, thus, how the line formation physics behaves for those variables; ii) it is a result of Galactic formation physics, where the more metal-poor clusters were enriched by different mechanisms than were the metal-rich clusters, thereby producing different [Ca/Fe] ratios as a function of [Fe/H] (see below); or, iii)  $[\text{Fe}/\text{H}]_{ZW84}$  is non-linear with respect to the true [Fe/H]. The non-linear relationship may well result from some combination of the preceding factors.

Our referee suggested that further insight might result from plotting [Ca/H] vs  $W'$ . To investigate this suggestion, we employed the abundance data in Carney’s (1996) critical compilation, where [Ca/Fe] as well as  $[\text{Fe}/\text{H}]_{zinn}$  and  $[\text{Fe}/\text{H}]_{spec}$  are given. The former [Fe/H] from Zinn (1985) is essentially the  $[\text{Fe}/\text{H}]_{ZW84}$  employed throughout this paper, while  $[\text{Fe}/\text{H}]_{spec}$  was computed by Carney from spectroscopic abundance determinations in the literature, which

---

<sup>6</sup>Note, however, that it is likely that all of our Ca II triplet measures are on the square-root portion of the curve of growth (A. Irwin, private communication), hence AD91’s suggestion may be incorrect.

he put onto a common scale of solar iron abundance. For the 18 clusters in common, we have computed  $[\text{Ca}/\text{H}]_{zinn} = [\text{Fe}/\text{H}]_{zinn} + [\text{Ca}/\text{Fe}]_{carney}$  and  $[\text{Ca}/\text{H}]_{spec} = [\text{Fe}/\text{H}]_{spec} + [\text{Ca}/\text{Fe}]_{carney}$ , where quantities on the right hand side are all from Carney’s review. These are shown in Figure 6, top and bottom, respectively. The linear regressions ( $[\text{Ca}/\text{H}]_{zinn} = 0.35W' - 2.36$ ,  $[\text{Ca}/\text{H}]_{spec} = 0.32W' - 2.23$ ), as well as the cubic relation found in §4.3 between  $W'$  and  $[\text{Fe}/\text{H}]_{ZW84}$ , are plotted in each panel. The dispersion about the linear regression of  $W'$  on  $[\text{Ca}/\text{H}]_{spec}$  is about half that of  $[\text{Ca}/\text{H}]_{zinn}$ , whose data suggest a quadratic or higher fit would be more appropriate. Moreover, on the  $W'$  interval in common with Norris, et al.’s (1996) Figure 7 for stars in  $\omega$  Cen, the agreement of their slope and intercept is within the uncertainties of our Figure 6 linear regressions.

From Figure 6,  $[\text{Ca}/\text{H}]_{spec}$  would seem to be linearly correlated with  $W'$  for these clusters. In turn, this would seem to imply that the non-linear relationship between  $W'$  and  $[\text{Fe}/\text{H}]_{ZW84}$  is not due predominantly to line formation physics. These initial impressions might be taken with some caution, however, because of (a) the caveats raised in Carney’s analysis, (b) the relatively small number of clusters in common, and (c) concerns about the unknown role of systematic effects in high dispersion analyses as a function of  $[\text{Fe}/\text{H}]$  (and from one investigator to another).

## 6.2. Galactic Formation and the $\alpha$ Elements

The foregoing raises important questions of what  $W'$  is actually measuring over the parameter range of the globular cluster RGB stars, and what it can tell us about the formation of the Milky Way. We briefly comment upon the second query here, and upon the first in the next section.

Carney (1996) has carefully reviewed spectroscopic determinations of  $[\alpha/\text{Fe}]$  in globular clusters. He concluded that the mean  $[\alpha/\text{Fe}]$  values determined from silicon and titanium do not appear to vary over the range of  $[\text{Fe}/\text{H}] = -2.24$  to  $-0.58$ , nor does  $[\text{O}/\text{Fe}]$  for those RGB stars which are presumed to be unmixed, and they are all strongly enhanced relative to solar values. That the  $\alpha$  elements appear to share a common, uniform enhancement among the globular clusters contrasts with the halo field star situation, in which  $[\text{O}/\text{Fe}]$  and  $[\alpha/\text{Fe}]$  are enhanced by  $+0.3$  to  $0.5$  dex for  $[\text{Fe}/\text{H}] \lesssim -1.4 \pm 0.3$  and then drop to solar values (e.g., Greenstein 1970, Wheeler, et al. 1989), in ways reminiscent of the relation between  $W'$  and  $[\text{Fe}/\text{H}]_{ZW84}$  in Figure 4. Interestingly, among the  $\alpha$  elements in globular cluster stars,  $[\text{Ca}/\text{Fe}]$  may behave more like  $[\alpha/\text{Fe}]$  in the field halo stars; however, Carney suggests that the observed decline of  $[\text{Ca}/\text{Fe}]$  as  $[\text{Fe}/\text{H}]$  increases may be an artifact arising from the use of neutral calcium lines to determine  $[\text{Ca}/\text{Fe}]$  in the available spectroscopic studies.

If, as Carney (1996) discusses, his interpretation of the fairly extensive HDS data available for globular clusters is correct, it suggests that, contrary to evidence from field halo star studies, contributions from supernovae of Type Ia are absent from the chemical evolution of the globular clusters or operated on a very different time scale than commonly thought. This conclusion

doubtless will be controversial, in part because of the contrasting field halo star patterns and in part because arguments exist for a smaller age range among the globular clusters than he advocates (see, e.g., Hesser 1995, Richer, et al. 1996, Stetson, Vandenberg & Bolte 1996, Hesser, et al. 1996b). Nonetheless, there is no doubt that the distribution of the  $\alpha$  elements provides a clue, perhaps critical, regarding how the Galactic halo formed and, thus, it is crucial to understand the limitations of the Ca II triplet as a metallicity indicator.

### 6.3. The Calcium Triplet as a Metallicity Surrogate

As reviewed in §2, the Ca II triplet has not always enjoyed its current popularity as a relatively easily determined surrogate for metallicity. For the Galactic globular clusters, others have demonstrated, and we have confirmed and extended, that the triplet appears to be a sensitive metallicity indicator. However, as noted in the preceding section, Carney (1996) raises concerns whether calcium participates in the uniform enhancement patterns exhibited by O, Si and Ti. If the Galactic halo formed by mergers of smaller galaxies that had undergone independent chemical evolution, element ratios could differ from one set of clusters to another according to the history of supernovae and the mixing of their ejecta in the galaxy of cluster origin.

For our own efforts to determine ages of the far outer halo clusters from Hubble Space Telescope photometry (cf. Hesser, et al. 1996a, Stetson, et al. 1996), detailed spectroscopic abundances will be quite challenging to obtain from high-dispersion spectra; consequently, high reliance is currently placed on the Ca II triplet as a metallicity surrogate. Should the outer halo clusters by and large represent a different family, it is possible that calcium (and the  $\alpha$  elements in general) may have followed a different enrichment path than clusters in the inner halo. Similar concerns might apply for other possible families of clusters throughout the Milky Way. Although little evidence for deviations from the Figure 4 mean relation is evident for some of the suggested subsystems of Galactic globular clusters, Brown et al. (1997) find from spectroscopic analysis of Rup 106 and Pal 12 that the  $\alpha$ -elements are *not* enhanced over the solar ratio. At least when interpreting Ca II triplet data for an individual globular cluster, we have strong evidence from color-magnitude diagrams that an internal age range does not factor into its abundance sensitivity. The same cannot be said when interpreting the results of Ca II triplet measurements in dwarf spheroidal galaxies (or other resolvable stellar populations where a range of ages and abundances are likely), nor, especially, when interpreting triplet strengths in composite light spectra. In such cases, additional observational constraints on the parameters that affect the formation of the triplet lines are required for reliable metallicities to be derived from them.

It seems particularly unfortunate that, in spite of the heavy reliance placed upon the calcium triplet in modern studies that strive to constrain the formation of the Galaxy through metallicity and age determinations of objects throughout the halo, no thorough modelling of the triplet lines has been carried out in a way that would help resolve some of the issues raised herein or by previous workers. To our knowledge, the most comprehensive theoretical work on the Ca II triplet

has been done by Jorgensen et al. (1992), but they only include calculations for  $[\text{Fe}/\text{H}] \geq -1$ , and they do not include the effects of line blanketing, which could play a significant role in depressing the pseudo-continuum for cool RGB stars in the more metal rich clusters. To help rectify this situation, we have begun some exploratory theoretical studies of the line formation physics for the Ca II triplet in collaboration with Ana Larson and Alan Irwin at the University of Victoria. We are theoretically simulating the AD91  $W'$  technique. Among our goals is to determine if a non-linear relationship between  $W'$  and  $[\text{Fe}/\text{H}]$  is expected from the line formation physics alone. The oxygen enhanced isochrones of Bergbusch and Vandenberg (1992) are used to define the  $\log(g) - T_{\text{eff}}$  loci of RGB stars in globular clusters with  $[\text{Fe}/\text{H}]$  ranging from 0 to  $-2$ . Full synthetic spectra calculations are then done using the Ssynth code (Larson and Irwin, 1996), and a reduction technique identical to that described in Paper I is applied to obtain  $W'$  values.

We strongly encourage other groups with the appropriate theoretical tools to examine independently this empirical diagnostic, whose relevance to many areas of Galactic and extragalactic astrophysics is growing steadily.

#### 6.4. Final Remarks

The globular cluster  $[\text{Fe}/\text{H}]$  scale is fundamental to our understanding of the age and chemical evolution of our Galaxy. For more than a decade, researchers have relied on the  $[\text{Fe}/\text{H}]$  scale of ZW84, which seems generally to provide adequate relative rankings (see §4), but depends on the non-homogeneous  $[\text{Fe}/\text{H}]$  scale of Frogel et al. (1983) for an absolute calibration (see §2). Although the scale of Frogel et al. (1983) was state of the art at the time, some of their data and analysis techniques are almost twenty years old, and deserve revisiting using subsequent improvements. The homogeneous analysis of good quality, high-dispersion spectra by CG97 appears to be an important first step in defining a modern high dispersion  $[\text{Fe}/\text{H}]$  scale. However, the CG97  $[\text{Fe}/\text{H}]$  scale creates a paradox, since it is unclear at the moment whether  $[\text{Fe}/\text{H}]_{\text{ZW84}}$  or  $[\text{Fe}/\text{H}]_{\text{CG97}}$  approximates the true  $[\text{Fe}/\text{H}]$  scale more closely. Since this issue is not likely to be resolved in the near future, we have transformed our  $W'$  values into  $[\text{Fe}/\text{H}]$  on both scales (see Table 2) so that researchers can perform their analysis using either.

G.A.R. acknowledges the valuable computer assistance offered by Daniel Durand, Gerry Justice, and Wes Fisher over the course of this project, as well as the National Research Council of Canada for an opportunity to work at DAO. We thank the anonymous referee for a helpful report.

## REFERENCES

- Alloin, D., and Bica, E. 1989, *A&A*, 217, 57
- Anderson, C.M. 1974, *ApJ*, 190, 585
- Armandroff, T.E. 1989, *AJ*, 97,375
- Armandroff, T.E., and Zinn, R. 1988, *AJ*, 96, 92 (AZ88)
- Armandroff, T.E., and Da Costa, G.S. 1991, *AJ*, 101, 1329 (AD91)
- Armandroff, T.E., Da Costa, G.S., and Zinn, R. 1992, *AJ*, 104, 164 (ADZ92)
- Brown, J. A., Wallerstein, G., and Oke, J.B. 1991, *AJ*, 101, 1693
- Brown, J. A., and Wallerstein, G. 1992, *AJ*, 104, 1818
- Brown, J. A., Wallerstein, G., and Zucker, D. 1996, Formation of the Galactic Halo ... Inside and Out, ASP Conference Series, Vol. 92, eds. Heather Morrison and Ata Sarajedini (San Francisco, ASP), p. 355
- Brown, J. A., Wallerstein, G., and Zucker, D. 1997, *AJ*, in press
- Bergbusch, P.A., and Vandenberg, D.A. 1992, *ApJS*, 81, 163
- Carney, B.W. 1996, *PASP*, 108, 900
- Carretta, E., and Gratton, R.G. 1997, *A&AS*, 121, 95 (CG97)
- Cohen, J.G. 1978, *ApJ*, 221, 788
- Cohen, J.G. 1978b, *ApJ*, 223, 487
- Cohen, J.G. 1979, *ApJ*, 228, 405
- Cohen, J.G. 1979b, *ApJ*, 231, 751
- Cohen, J.G. 1980, *ApJ*, 241, 981
- Cohen, J.G. 1981, *ApJ*, 247, 869
- Cohen, J.G. 1982, *ApJ*, 258, 143
- Cohen, J.G. 1983, *ApJ*, 270, 654
- Cohen, J.G., and Sleeper, C. 1995, *AJ*, 109, 242
- Cohen, J.G., and Frogel, J.A. 1982, *ApJ*, 255 L39
- Da Costa, G.S., and Armandroff, T.E. 1995, *AJ*, 109, 2533 (DA95)
- Da Costa, G.S., Armandroff, T.E. , and Norris, J.E. 1992, *AJ*, 104, 154 (DAN92)
- Da Costa, G.S., and Seitzer, P. 1989, *AJ*, 97, 405
- Diaz, A.I., Terlevich, E., and Terlevich, R. 1989, *MNRAS*, 239, 325
- Freeman, K.C., and Norris, J. 1981, *ARA&A*, 19, 319

- Frogel, J.A., Cohen, J.G., Persson, S.E. 1983, *ApJ*, 275, 773
- Geisler, D., Piatti, A.E., Clariá, J., and Minniti, D. 1995, *AJ*, 109, 605 (G95)
- Gratton, R.G., and Ortolani, S. 1989, *A&A*, 211, 41 (GO89)
- Greenstein, J.L. 1970, *Comm. Astrophys. Space Sci.*, 2, 85
- Harris, W.E. 1994, electronically published catalog, McMaster University
- Hesser, J.E. 1995, in *Stellar Populations*, eds. G. Gilmore, P. Van der Kruit (Dordrecht, Kluwer), p. 51
- Hesser, J.E., Stetson, P.B., McClure, R.D., van den Bergh, S., Harris, W.E., Bolte, M., VandenBerg, D.A., Bond, H.E., Fahlman, G.G., Richer, H.B., Bell, R.A. 1996a, *BAAS*, 28, 1363.
- Hesser, J.E., Stetson, P.B., Harris, W.E., Bolte, M., Smecker-Hane, T.A., VandenBerg, D.A., Bell, R.A., Bond, H.E., van den Bergh, S., McClure, R.D., Fahlman, G.G., and Richer, H.B. 1996b, *J. Korean Astron. Soc.*, 29, S111.
- Jones, J.E., Alloin, D.M., and Jones, B.J.T. 1984, *ApJ*, 184, 787
- Jorgensen, U.G., Carlsson, M., and Johnson, H.R. 1992, *A&A*, 254, 258
- Kraft, R.P. 1979, *ARA&A*, 17, 309
- Kraft, R.P., Sneden, C., Langer, G.E., Shetrone, M.D. 1993, *AJ*, 106, 1490
- Kraft, R.P., Sneden, C., Langer, G.E., Shetrone, M.D., Bolte, M. 1995, *AJ*, 109, 2586
- Kurucz, R.L. 1992, private communication
- Larson, A.M. and Irwin, A.W. 1996, *A&AS*, 117, 189L
- Lee, Y-W, Demarque, P., and Zinn, R. 1994, *ApJ*, 423, 248
- Manduca, A. 1983, *BAAS*, 15, 647.
- Menzies, J. 1974, *MNRAS*, 169, 79
- Minniti, D., Geisler, D., Peterson, R.C., Claria, J.J. 1993, *ApJ*, 413, 548 (M93)
- Norris, J.E., Freeman, K.C. and Mighell, K.J. 1996, *ApJ*, 462, 241
- Olszewski, E.W., Schommer, R.A., Suntzeff, N.B., and Harris, H. 1991, *AJ*, 101, 515
- Pilachowski, C.A., Canterna, R., Wallerstein, G. 1980, *ApJ*, 235, L21
- Richer, H.B. et al. 1996, *ApJ*, 463, 602
- Rutledge, G.A., Hesser, J.E., Stetson, P.B., Mateo, M., Simard, L., Bolte, M., Friel, E.D., and Copin, Y. 1997, *PASP*, submitted (Paper I)
- Sandage, A., and Wildey, R. 1967, *ApJ*, 150, 469
- Sarajedini, A., and Norris, J.E. 1994, *ApJS*, 93, 161



- Smith, H.A. 1984, ApJ, 281, 148
- Sneden, C., Kraft, R.P., Prosser, C.F., and Langer, G.E. 1991, AJ, 102, 2001
- Sneden, C., Kraft, R.P., Prosser, C.F., and Langer, G.E. 1992, AJ, 104, 2121
- Sneden, C., Kraft, R.P., Langer, G.E., Prosser, C.F., and Shetrone, M.D. 1994, AJ, 107, 1773
- Spinrad, H., and Taylor, B.J. 1969, ApJ, 157, 1279
- Spinrad, H., and Taylor, B.J. 1971, ApJS, 22, 445
- Stetson, P.B. 1989, Image and Data Processing, eds. B Barbuy, E. Janot-Pacheco, A. M. Magalhães, S.M. Viegas, published by Departamento Astronomia, Instituto Astronomico e Geofísico, Universidade de São Paulo, C.P. 9638, São Paulo 01065, Brazil.
- Stetson, P.B., Hesser, J.E., McClure, R.D., van den Bergh, S., Bolte, M., Harris, W.E., VandenBerg, D.A., Bond, H.E., Fahlman, G.G., Richer, H.B., Bell, R.A. 1996, BAAS, 28, 1362.
- Stetson, P.B., VandenBerg, D.A., and Bolte, M. 1996, PASP, 108, 560
- Suntzeff, N.B., Schommer, R.A., Olszewski, E.W., Walker, A.R. 1992, AJ, 104 (5), 1743 (S92)
- Suntzeff, N.B., Mateo, M., Terndrup, D.M., Olszewski, E.W., Geisler, D., and Weller, W. 1993, ApJ, 418, 208 (S93)
- Suntzeff, N.B., and Kraft, R.P. 1996, AJ, 111, 1913 (SK96)
- van den Bergh, S., 1965, JRASC, 59, 151
- van den Bergh, S., 1967, AJ, 72, 70
- van den Bergh, S., 1993, AJ, 105, 971
- Wheeler, J.C., Sneden, C., and Truran, J.W. 1989, ARA&A, 27, 279
- Zinn, R. 1980a, ApJ, 241, 602
- Zinn, R. 1980b, ApJS, 42, 19
- Zinn, R. 1985, ApJ, 293, 424
- Zinn, R., and West, M.J. 1984, ApJS, 55, 45 (ZW84)

Fig. 1.— The linear regression used to convert the  $W'$  values of DA95 into  $W'$  values on the Paper I system. The cluster NGC 5927, plotted as an open circle, was not used to determine the regression.

Fig. 2.— A comparison of the four indices used by ZW84 to construct their spectroscopically augmented  $Q_{39}$  index. Note that the bottom right panel is the original photometric  $Q_{39}$  of Zinn (1980b). Typical error bars are given in the upper left corner of each plot. An error bar is attached to an individual point only if its uncertainty exceeds the typical value. The different symbols denote Lee et al. (1994) HB types as follows: *solid circles* (R):  $(B - R)/(B + V + R) \leq -0.5$ ; *solid squares* (r):  $-0.5 < (B - R)/(B + V + R) \leq 0.0$ ; *open diamonds* (b):  $0.0 < (B - R)/(B + V + R) \leq 0.5$ ; *open triangles* (B):  $0.5 < (B - R)/(B + V + R)$ ;  $\times$ :  $(B - R)/(B + V + R)$  is undefined. The letters R, r, b, and B are used in the figure legend as a reminder of the HB type. The *open circles* in the upper left plot are overlaid on clusters for which the Ca II K equivalent widths have less than average weight (as defined by ZW84).

Fig. 3.— A comparison of the spectroscopically augmented  $[\text{Fe}/\text{H}]_{Q_{39}}$  defined by ZW84, which is a combination of photometric  $Q_{39}$  and transformed, low-dispersion spectral indices (upper panel), and  $[\text{Fe}/\text{H}]_{avg}$  defined using the average of an assortment of indices (middle panel). The bottom panel shows the difference,  $[\text{Fe}/\text{H}]_{Q_{39}} - [\text{Fe}/\text{H}]_{avg}$ . All  $[\text{Fe}/\text{H}]$  values have been taken from Table 5 of ZW84. The symbols are defined as in Figure 2, except for the *open circles* which, in this plot, are overlaid on clusters for which  $[\text{Fe}/\text{H}]_{avg}$  was obtained using only one index.

Fig. 4.— The  $[\text{Fe}/\text{H}]$  values from Table 6 of ZW84 have been plotted against our calcium index,  $W'$ . The upper panel contains only clusters for which  $[\text{Fe}/\text{H}]_{ZW84}$  was derived from a combination of  $[\text{Fe}/\text{H}]_{Q_{39}}$  and  $[\text{Fe}/\text{H}]_{avg}$  (see Figure 3). These clusters were used to fit a cubic polynomial, plotted as a solid line, which is then used to define the most probable value of  $[\text{Fe}/\text{H}]$  and  $W'$  for each cluster on the ZW84 scale. NGC 1851, plotted as an open circle, was not used in the regression. The dotted line, which abruptly changes slope at  $W' = 3.64 \text{ \AA}$ , is the calibrating line of DA95 transformed to our Paper I system. The lower panel shows all clusters that are in common to the two studies, where the symbols are defined as follows: *solid circles* when  $[\text{Fe}/\text{H}]_{ZW84}$  was derived from a combination of  $[\text{Fe}/\text{H}]_{Q_{39}}$  and  $[\text{Fe}/\text{H}]_{avg}$ ; *squares* when  $[\text{Fe}/\text{H}]_{ZW84}$  was derived from  $[\text{Fe}/\text{H}]_{Q_{39}}$  only; *diamonds* when  $[\text{Fe}/\text{H}]_{ZW84}$  was derived from  $[\text{Fe}/\text{H}]_{Q_{39}}$  only, where  $Q_{39}$  was calculated using only the photometric  $Q_{39}$  index; *triangles* when  $[\text{Fe}/\text{H}]_{ZW84}$  was derived from  $[\text{Fe}/\text{H}]_{avg}$  only;  $\times$  when  $[\text{Fe}/\text{H}]_{ZW84}$  was derived from some other, presumably less reliable, index. The *open circles* are overlaid on clusters which van den Bergh (1993) defines as having retrograde motions about the Galaxy. The error bars in the upper left corner represent errors of  $\pm 0.15$  dex in  $[\text{Fe}/\text{H}]_{ZW84}$ , and  $\pm 0.15 \text{ \AA}$  in  $W'$ . Error bars are attached to the symbols only if they exceed these values. The solid and dotted lines are reproduced from the top panel.

Fig. 5.— The  $[\text{Fe}/\text{H}]$  values from Cohen, and from five more recent high-dispersion spectroscopy studies, are compared to the most probable  $\langle W' \rangle$  index listed in Table 2. The error bars in the upper left corner give the typical errors for each of the quantities. The solid line in each panel is

the cubic fit to  $[\text{Fe}/\text{H}]_{ZW84}$  from Figure 4. The dotted line in the CG97 panel shows the linear regression used to transform the  $\langle W' \rangle$  values to  $[\text{Fe}/\text{H}]_{CG97}$ .

Fig. 6.— A comparison of  $[\text{Ca}/\text{H}]$  with our  $W'$  measurements; see text for details.

Rutledge et al.: GGC CaII Metallicity Scale. II Analysis. — Figure 1.

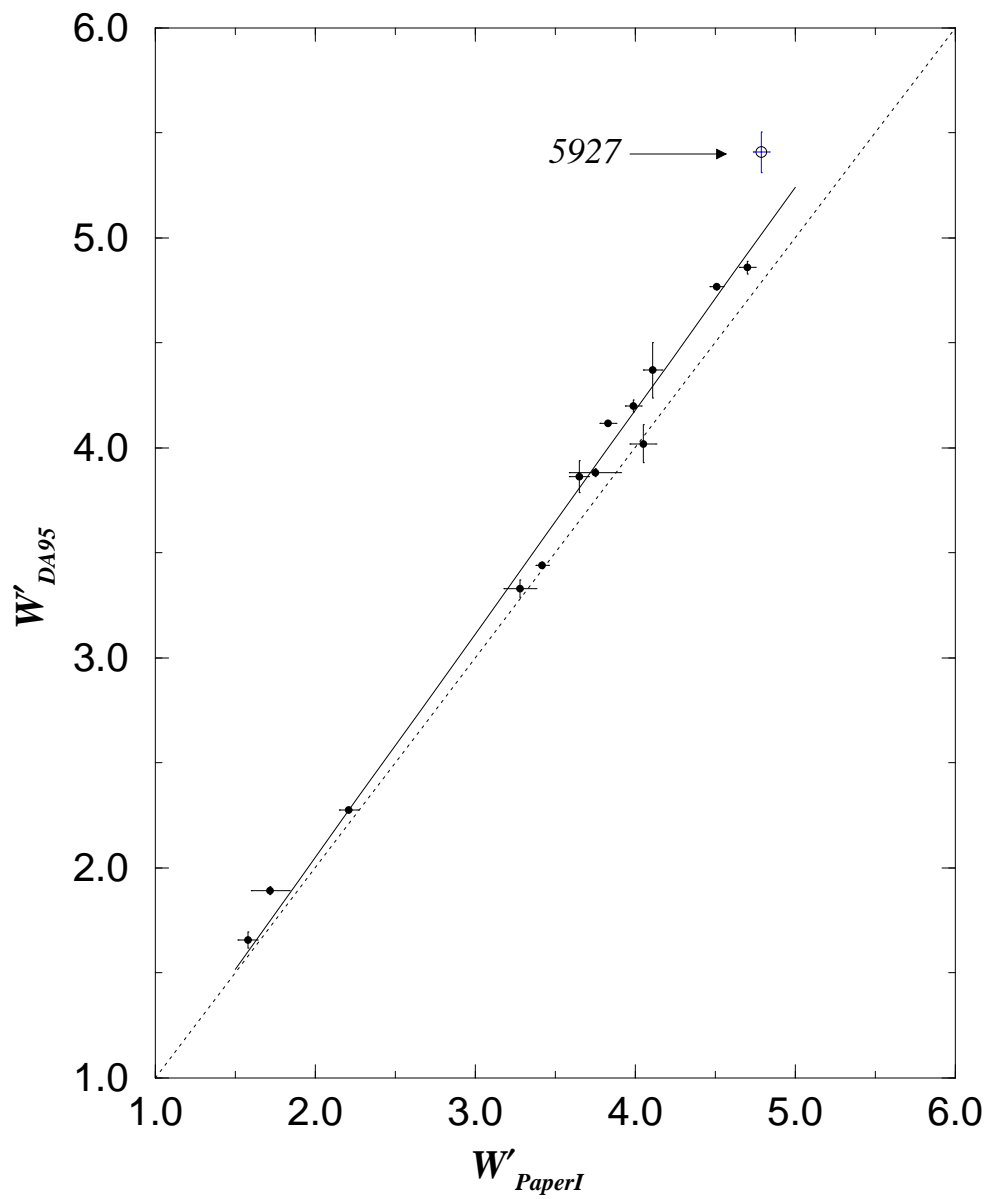


TABLE 1. Compilation of Cluster  $W'$  Values

No.	NGC	Name	IAU	$W'_{PaperI}$	$W'_{DA95}$	$W'_{Other}$	$W'_{Adopted}$	ref
1	104	47 Tuc	C0021-723	4.51±0.04	4.55±0.15	4.54±0.03	4.53± 0.07	SK96
2	288		C0050-268	3.65±0.06	3.70±0.15	...	3.66± 0.08	
3	362		C0100-711	3.72±0.07	...	...	3.72± 0.09	
4	1261		C0310-554	3.77±0.09	...	...	3.77± 0.11	
5		Eridanus	C0422-213	...	...	3.47±0.22	3.47± 0.23	AD91
6	1851		C0512-400	...	4.19±0.14	...	4.19± 0.16	
7	1904		C0522-245	...	3.11±0.12	...	3.11± 0.14	
8	2298		C0647-359	2.24±0.05	...	2.38±0.10	2.27± 0.09	G95
9	2808		C0911-646	3.75±0.08	...	...	3.75± 0.10	
10		Pal 3	C1003+003	...	...	3.09±0.25	3.09± 0.26	ADZ92
11	3201		C1015-461	3.41±0.03	...	3.45±0.03	3.43± 0.07	SK96
12		Pal 4	C1126+292	...	...	3.64±0.25	3.64± 0.26	ADZ92
13	4147		C1207+188	...	...	2.80±0.14	2.80± 0.14	ADZ92
14	4372		C1223-724	1.94±0.05	...	1.70±0.08	1.87± 0.13	G95
15		Rup 106	C1235-509	...	...	2.81±0.12	2.81± 0.12	DAN92
16	4590	M 68	C1236-264	1.58±0.06	1.62±0.11	...	1.59± 0.08	
17	4833		C1256-706	2.27±0.05	...	2.25±0.09	2.27± 0.08	G95
18	5053		C1313+179	...	...	1.67±0.13	1.67± 0.14	G95
19	5286		C1343-511	3.03±0.08	...	...	3.03± 0.10	
20	5694		C1436-263	...	...	2.20±0.16	2.20± 0.17	G95
21	5897		C1514-208	2.24±0.07	...	2.05±0.08	2.16± 0.11	G95
22	5904	M 5	C1516+022	3.75±0.16	3.72±0.13	...	3.73± 0.12	
23	5927		C1524-505	4.79±0.05	5.16±0.18	...	4.82± 0.11	
24	5986		C1542-376	3.16±0.09	...	...	3.16± 0.11	
25		Pal 14	C1608+150	...	...	3.11±0.22	3.11± 0.23	ADZ92
26	6093	M 80	C1614-228	2.86±0.06	...	...	2.86± 0.09	
27	6101		C1620-720	1.95±0.11	...	2.26±0.11	2.11± 0.17	G95
28	6121	M 4	C1620-264	3.83±0.05	3.94±0.13	3.90±0.05	3.87± 0.07	SK96
29	6144		C1624-259	2.20±0.05	...	2.24±0.11	2.21± 0.08	G95
30	6171	M 107	C1629-129	3.99±0.05	4.02±0.14	...	3.99± 0.08	
31	6205	M 13	C1639+365	...	3.27±0.15	...	3.27± 0.17	
32	6218	M 12	C1644-018	3.85±0.10	...	3.70±0.06	3.74± 0.09	S93
33	6235		C1650-220	3.54±0.11	...	...	3.54± 0.13	
34	6254	M 10	C1654-040	3.42±0.07	...	...	3.42± 0.09	
35		Pal 15	C1657-004	...	2.05±0.14	...	2.05± 0.15	
36	6266	M 62	C1658-300	3.95±0.07	...	...	3.95± 0.09	
37	6273	M 19	C1659-262	2.69±0.10	...	...	2.69± 0.12	
38	6304		C1711-294	4.84±0.05	...	...	4.84± 0.08	
39	6352		C1721-484	4.73±0.07	...	...	4.73± 0.09	
40	6366		C1725-050	4.70±0.05	4.64±0.15	...	4.69± 0.08	
41	6362		C1726-670	3.93±0.07	...	...	3.93± 0.09	
42	6397		C1736-536	2.21±0.06	2.21±0.11	2.12±0.06	2.17± 0.08	SK96
43	6496		C1755-442	4.70±0.08	...	...	4.70± 0.10	
44	6522		C1800-300	3.47±0.09	...	...	3.47± 0.11	
45	6535		C1801-003	2.74±0.27	...	...	2.74± 0.28	
46	6528		C1801-300	5.41±0.14	...	...	5.41± 0.15	
47	6544		C1804-250	3.53±0.09	...	...	3.53± 0.11	
48	6541		C1804-437	2.72±0.05	...	...	2.72± 0.08	

TABLE 1. (continued)

No.	NGC	Name	IAU	$W'_{PaperI}$	$W'_{DA95}$	$W'_{Other}$	$W'_{Adopted}$	ref
49	6553		C1806-259	5.13±0.09	...	...	5.13± 0.11	
50	6624		C1820-303	4.66±0.05	...	...	4.66± 0.08	
51	6626		C1821-249	4.05±0.08	3.85±0.16	...	4.01± 0.10	
52	6638		C1827-255	4.31±0.10	...	...	4.31± 0.12	
53	6637	M 69	C1828-323	4.48±0.07	...	...	4.48± 0.09	
54	6681	M 70	C1840-323	3.14±0.05	...	...	3.14± 0.08	
55	6712		C1850-087	4.11±0.06	4.18±0.19	...	4.12± 0.09	
56	6715	M 54	C1851-305	...	3.32±0.18	...	3.32± 0.19	
57	6717	Pal 9	C1852-227	3.78±0.11	...	...	3.78± 0.13	
58	6723		C1856-367	4.07±0.08	...	...	4.07± 0.10	
59	6752		C1906-600	3.42±0.04	3.30±0.12	...	3.41± 0.07	
60		Ter 7	C1914-347	...	5.05±0.16	...	5.05± 0.17	
61		Arp 2	C1925-304	...	2.90±0.21	...	2.90± 0.22	
62	6809	M 55	C1936-310	2.69±0.05	...	...	2.69± 0.08	
63		Ter 8	C1938-341	...	2.07±0.12	...	2.07± 0.14	
64		Pal 11	C1942-081	...	...	4.99±0.30	4.99± 0.31	ADZ92
65	6838	M 71	C1951+186	...	4.64±0.16	...	4.64± 0.17	
66	6981	M 72	C2050-127	3.53±0.10	...	...	3.53± 0.12	
67	7078	M 15	C2127+119	...	1.56±0.10	...	1.56± 0.12	
68	7089	M 2	C2130-010	3.28±0.10	3.20±0.13	...	3.25± 0.10	
69	7099	M 30	C2137-234	1.72±0.12	1.84±0.11	...	1.79± 0.10	
70		Pal 12	C2143-214	4.57±0.15	...	4.53±0.16	4.55± 0.13	AD91
71	7492		C2305-159	2.98±0.16	...	...	2.98± 0.17	

Notes to Table 1.

We did not include ADZ92's data for NGC 5053 ( $W'_{PaperI} = 1.62 \pm 0.14$ ) and M 92 ( $W'_{PaperI} = 1.82 \pm 0.09$ ) since the  $\sum C\alpha$  values for these clusters would require a large extrapolation of the ADZ92 transformation equation defined in Paper I.

Rutledge et al.: GGC CaII Metallicity scale. II Analysis — Figure 2

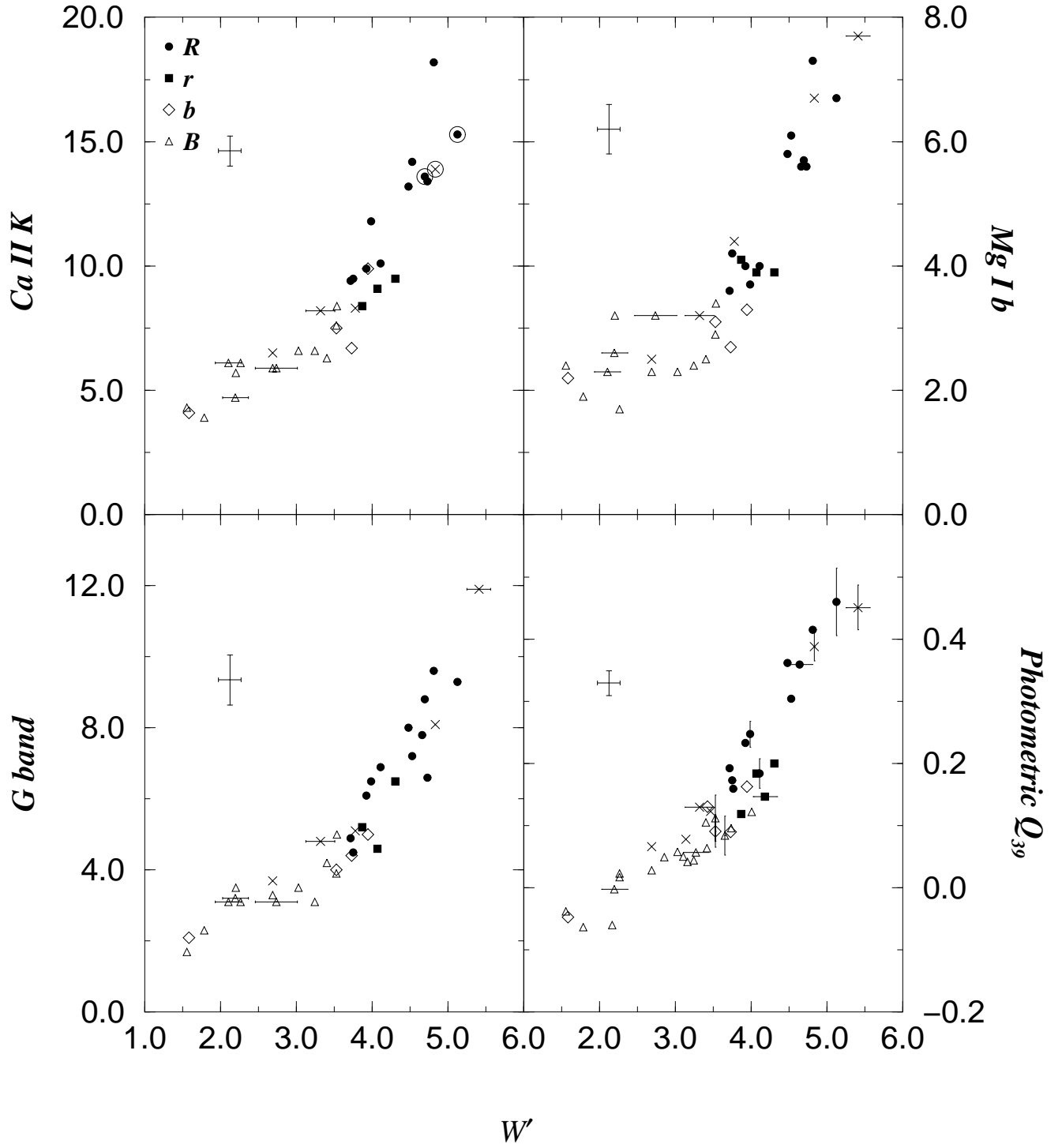


TABLE 2. Compilation of Cluster  $[\text{Fe}/\text{H}]$  Values

NGC	Name	$[\text{Fe}/\text{H}]_{ZW84}^a$	$\langle W' \rangle$	$\langle [\text{Fe}/\text{H}]_{ZW84} \rangle^b$	$[\text{Fe}/\text{H}]_{CG97}^c$	notes
104	47 Tuc	$-0.71 \pm 0.08$	$4.53 \pm 0.05$	$-0.71 \pm 0.05$	$-0.78 \pm 0.02$	
288		$-1.40 \pm 0.12$	$3.66 \pm 0.08$	$-1.40 \pm 0.05$	$-1.14 \pm 0.03$	
362		$-1.27 \pm 0.07$	$3.78 \pm 0.07$	$-1.33 \pm 0.05$	$-1.09 \pm 0.03$	
1261		$-1.29 \pm 0.09$	$3.80 \pm 0.09$	$-1.32 \pm 0.06$	$-1.08 \pm 0.04$	
	Eridanus	$-1.35 \pm 0.30$	$3.51 \pm 0.21$	$-1.48 \pm 0.11$	$-1.20 \pm 0.09$	
1851		$-1.33 \pm 0.09$	$3.93 \pm 0.15$	$-1.23 \pm 0.11$	$-1.03 \pm 0.06$	3
1904		$-1.68 \pm 0.09$	$3.09 \pm 0.12$	$-1.67 \pm 0.05$	$-1.37 \pm 0.05$	
2298		$-1.81 \pm 0.11$	$2.28 \pm 0.08$	$-1.91 \pm 0.02$	$-1.71 \pm 0.03$	
2808		$-1.37 \pm 0.09$	$3.74 \pm 0.08$	$-1.36 \pm 0.05$	$-1.11 \pm 0.03$	
	Pal 3	$-1.78 \pm 0.30$	$3.06 \pm 0.25$	$-1.68 \pm 0.09$	$-1.39 \pm 0.10$	
3201		$-1.56 \pm 0.12$	$3.42 \pm 0.06$	$-1.53 \pm 0.03$	$-1.24 \pm 0.03$	
	Pal 4	$-2.20 \pm 0.40$	$3.48 \pm 0.37$	$-1.50 \pm 0.18$	$-1.21 \pm 0.15$	3
4147		$-1.80 \pm 0.26$	$2.80 \pm 0.14$	$-1.77 \pm 0.04$	$-1.50 \pm 0.06$	6
4372		$-2.08 \pm 0.15$	$1.86 \pm 0.12$	$-2.03 \pm 0.03$	$-1.88 \pm 0.05$	
	Rup 106	...	$2.81 \pm 0.12$	$-1.77 \pm 0.04$	$-1.49 \pm 0.05$	
4590	M 68	$-2.09 \pm 0.11$	$1.59 \pm 0.08$	$-2.11 \pm 0.03$	$-2.00 \pm 0.03$	
4833		$-1.86 \pm 0.09$	$2.28 \pm 0.08$	$-1.92 \pm 0.02$	$-1.71 \pm 0.03$	
5053		$-2.58 \pm 0.27$	$1.63 \pm 0.23$	$-2.10 \pm 0.07$	$-1.98 \pm 0.09$	
5286		$-1.79 \pm 0.11$	$3.00 \pm 0.10$	$-1.70 \pm 0.03$	$-1.41 \pm 0.04$	
5694		$-1.92 \pm 0.15$	$2.21 \pm 0.16$	$-1.93 \pm 0.04$	$-1.74 \pm 0.07$	
5897		$-1.68 \pm 0.11$	$2.23 \pm 0.18$	$-1.93 \pm 0.05$	$-1.73 \pm 0.07$	
5904	M 5	$-1.40 \pm 0.06$	$3.69 \pm 0.08$	$-1.38 \pm 0.05$	$-1.12 \pm 0.03$	
5927		$-0.30 \pm 0.09$	$4.85 \pm 0.06$	$-0.32 \pm 0.08$	$-0.64 \pm 0.02$	1,2
5986		$-1.67 \pm 0.10$	$3.15 \pm 0.10$	$-1.65 \pm 0.04$	$-1.35 \pm 0.04$	
	Pal 14	$-1.47 \pm 0.30$	$3.15 \pm 0.22$	$-1.65 \pm 0.09$	$-1.35 \pm 0.09$	
6093	M 80	$-1.68 \pm 0.12$	$2.87 \pm 0.09$	$-1.75 \pm 0.03$	$-1.47 \pm 0.04$	
6101		$-1.81 \pm 0.15$	$2.15 \pm 0.16$	$-1.95 \pm 0.04$	$-1.76 \pm 0.07$	
6121	M 4	$-1.28 \pm 0.10$	$3.87 \pm 0.07$	$-1.27 \pm 0.04$	$-1.05 \pm 0.03$	
6144		$-1.75 \pm 0.15$	$2.22 \pm 0.08$	$-1.93 \pm 0.02$	$-1.74 \pm 0.03$	
6171	M 107	$-0.99 \pm 0.06$	$4.12 \pm 0.09$	$-1.09 \pm 0.07$	$-0.95 \pm 0.04$	3
6205	M 13	$-1.65 \pm 0.06$	$3.20 \pm 0.11$	$-1.63 \pm 0.04$	$-1.33 \pm 0.05$	
6218	M 12	$-1.61 \pm 0.12$	$3.66 \pm 0.12$	$-1.40 \pm 0.07$	$-1.14 \pm 0.05$	
6235		$-1.40 \pm 0.15$	$3.56 \pm 0.12$	$-1.46 \pm 0.06$	$-1.18 \pm 0.05$	
6254	M 10	$-1.60 \pm 0.08$	$3.38 \pm 0.08$	$-1.55 \pm 0.04$	$-1.25 \pm 0.03$	
	Pal 15	...	$2.05 \pm 0.15$	$-1.98 \pm 0.04$	$-1.81 \pm 0.06$	
6266	M 62	$-1.29 \pm 0.15$	$3.93 \pm 0.09$	$-1.23 \pm 0.06$	$-1.02 \pm 0.04$	
6273	M 19	$-1.68 \pm 0.15$	$2.71 \pm 0.12$	$-1.80 \pm 0.03$	$-1.53 \pm 0.05$	
6304		$-0.59 \pm 0.23$	$4.81 \pm 0.07$	$-0.38 \pm 0.09$	$-0.66 \pm 0.03$	2
6352		$-0.51 \pm 0.08$	$4.71 \pm 0.05$	$-0.50 \pm 0.07$	$-0.70 \pm 0.02$	
6366		$-0.99 \pm 0.25$	$4.64 \pm 0.12$	$-0.58 \pm 0.14$	$-0.73 \pm 0.05$	
6362		$-1.08 \pm 0.09$	$4.01 \pm 0.07$	$-1.18 \pm 0.06$	$-0.99 \pm 0.03$	
6397		$-1.91 \pm 0.14$	$2.17 \pm 0.07$	$-1.94 \pm 0.02$	$-1.76 \pm 0.03$	
6496		$-0.48 \pm 0.15$	$4.71 \pm 0.08$	$-0.50 \pm 0.09$	$-0.70 \pm 0.03$	2
6522		$-1.44 \pm 0.15$	$3.49 \pm 0.10$	$-1.50 \pm 0.05$	$-1.21 \pm 0.04$	
6535		$-1.75 \pm 0.15$	$2.77 \pm 0.24$	$-1.78 \pm 0.07$	$-1.51 \pm 0.10$	
6528		$0.12 \pm 0.21$	...	...	...	4
6544		$-1.56 \pm 0.15$	$3.51 \pm 0.10$	$-1.48 \pm 0.05$	$-1.20 \pm 0.04$	
6541		$-1.83 \pm 0.15$	$2.72 \pm 0.08$	$-1.79 \pm 0.02$	$-1.53 \pm 0.03$	



TABLE 2. (continued)

NGC	Name	[Fe/H] <sub>ZW84</sub> <sup>a</sup>	$\langle W' \rangle$	$\langle [\text{Fe}/\text{H}]_{\text{ZW84}} \rangle$ <sup>b</sup>	[Fe/H] <sub>CG97</sub> <sup>c</sup>	notes
6553		$-0.29 \pm 0.11$	$4.96 \pm 0.08$	$-0.18 \pm 0.12$	$-0.60 \pm 0.04$	1,2,3
6624		$-0.35 \pm 0.15$	$4.71 \pm 0.07$	$-0.50 \pm 0.08$	$-0.70 \pm 0.03$	
6626		$-1.44 \pm 0.15$	$3.93 \pm 0.11$	$-1.23 \pm 0.08$	$-1.03 \pm 0.05$	
6638		$-1.15 \pm 0.15$	$4.22 \pm 0.10$	$-1.00 \pm 0.09$	$-0.90 \pm 0.04$	
6637	M 69	$-0.59 \pm 0.19$	$4.51 \pm 0.08$	$-0.72 \pm 0.09$	$-0.78 \pm 0.03$	
6681	M 70	$-1.51 \pm 0.14$	$3.16 \pm 0.08$	$-1.64 \pm 0.03$	$-1.35 \pm 0.03$	
6712		$-1.01 \pm 0.14$	$4.14 \pm 0.08$	$-1.07 \pm 0.06$	$-0.94 \pm 0.03$	
6715	M 54	$-1.43 \pm 0.15$	$3.40 \pm 0.16$	$-1.54 \pm 0.08$	$-1.25 \pm 0.07$	
6717	Pal 9	$-1.32 \pm 0.15$	$3.78 \pm 0.11$	$-1.33 \pm 0.07$	$-1.09 \pm 0.05$	
6723		$-1.09 \pm 0.14$	$4.08 \pm 0.09$	$-1.12 \pm 0.07$	$-0.96 \pm 0.04$	
6752		$-1.54 \pm 0.09$	$3.41 \pm 0.07$	$-1.54 \pm 0.03$	$-1.24 \pm 0.03$	
	Ter 7	...	$5.05 \pm 0.17$	$-0.05 \pm 0.26$	$-0.56 \pm 0.07$	1,2
	Arp 2	...	$2.90 \pm 0.22$	$-1.74 \pm 0.07$	$-1.45 \pm 0.09$	
6809	M 55	$-1.82 \pm 0.15$	$2.69 \pm 0.08$	$-1.80 \pm 0.02$	$-1.54 \pm 0.03$	
	Ter 8	...	$2.07 \pm 0.14$	$-1.97 \pm 0.04$	$-1.80 \pm 0.06$	
	Pal 11	$-0.70 \pm 0.40$	$4.77 \pm 0.22$	$-0.43 \pm 0.28$	$-0.68 \pm 0.09$	2,3
6838	M 71	$-0.58 \pm 0.08$	$4.64 \pm 0.06$	$-0.58 \pm 0.07$	$-0.73 \pm 0.03$	
6981	M 72	$-1.54 \pm 0.09$	$3.49 \pm 0.10$	$-1.50 \pm 0.05$	$-1.21 \pm 0.04$	
7078	M 15	$-2.15 \pm 0.08$	$1.54 \pm 0.11$	$-2.13 \pm 0.04$	$-2.02 \pm 0.04$	2
7089	M 2	$-1.62 \pm 0.07$	$3.24 \pm 0.09$	$-1.61 \pm 0.04$	$-1.31 \pm 0.04$	
7099	M 30	$-2.13 \pm 0.13$	$1.78 \pm 0.10$	$-2.05 \pm 0.03$	$-1.92 \pm 0.04$	
	Pal 12	$-1.14 \pm 0.20$	$4.41 \pm 0.16$	$-0.82 \pm 0.16$	$-0.83 \pm 0.06$	3
7492		$-1.51 \pm 0.30$	$3.00 \pm 0.17$	$-1.70 \pm 0.06$	$-1.41 \pm 0.07$	

<sup>a</sup>The corrections suggested by Zinn (1985) have been applied to these values. The errors are still taken from ZW84.

<sup>b</sup>This is our estimate of the most probable [Fe/H] value on the ZW84 scale, as calculated in §4.3.

<sup>c</sup>This is our estimate of the [Fe/H] value on the CG97 scale, as calculated in §5.

Notes to Table 2.

1. The  $\langle [\text{Fe}/\text{H}]_{\text{ZW84}} \rangle$  and  $\langle W' \rangle$  estimates for these cluster are less reliable than other clusters due to the lack of high quality metal rich calibrating clusters. 2. These [Fe/H]<sub>CG97</sub> values have been extrapolated past either the most metal poor calibrating cluster, NGC 4590, or the most metal rich calibrating cluster, NGC 6352 (see Table 3). 3. For these clusters, [Fe/H]<sub>CG97</sub> changes by more than 0.05 dex if the measured  $W'$  values are used in the calibration rather than the most probable  $\langle W' \rangle$  values, as is presented in column 6 above. The [Fe/H]<sub>CG97</sub> would change as follows, NGC 1851:  $-0.92 \pm 0.06$ , Pal 4:  $-1.14 \pm 0.11$ , NGC 6171  $\equiv$  M 107:  $-1.00 \pm 0.03$ , NGC 6553:  $-0.54 \pm 0.04$ , Pal 11:  $-0.59 \pm 0.13$ , Pal 12:  $-0.77 \pm 0.05$ . 4. NGC 6528 was not used in our analysis since its  $W'$  value lies beyond the last cluster used to fit the cubic polynomial between  $W'$  and [Fe/H]<sub>ZW84</sub>. It is clearly the most metal rich cluster in our sample. Using a rather large extrapolation of the measured  $W'$  calibration (see note 3), its  $W'$  value of  $5.41 \pm 0.15$  implies that [Fe/H]<sub>CG97</sub> =  $-0.42 \pm 0.06$ . 6. This cluster is not plotted in any of the graphs of this paper, nor is it used for any of the fitting since ZW84 did not include any  $Q_{39}$  data for this cluster despite the fact that they list a [Fe/H]<sub>Q<sub>39</sub></sub> in their Table 5. However, if it was plotted in our Figure 4, then it would lie very close to our derived calibration equation.

Rutledge et al.: GGC CaII Metallicity Scale. II Analysis -- Figure 3.

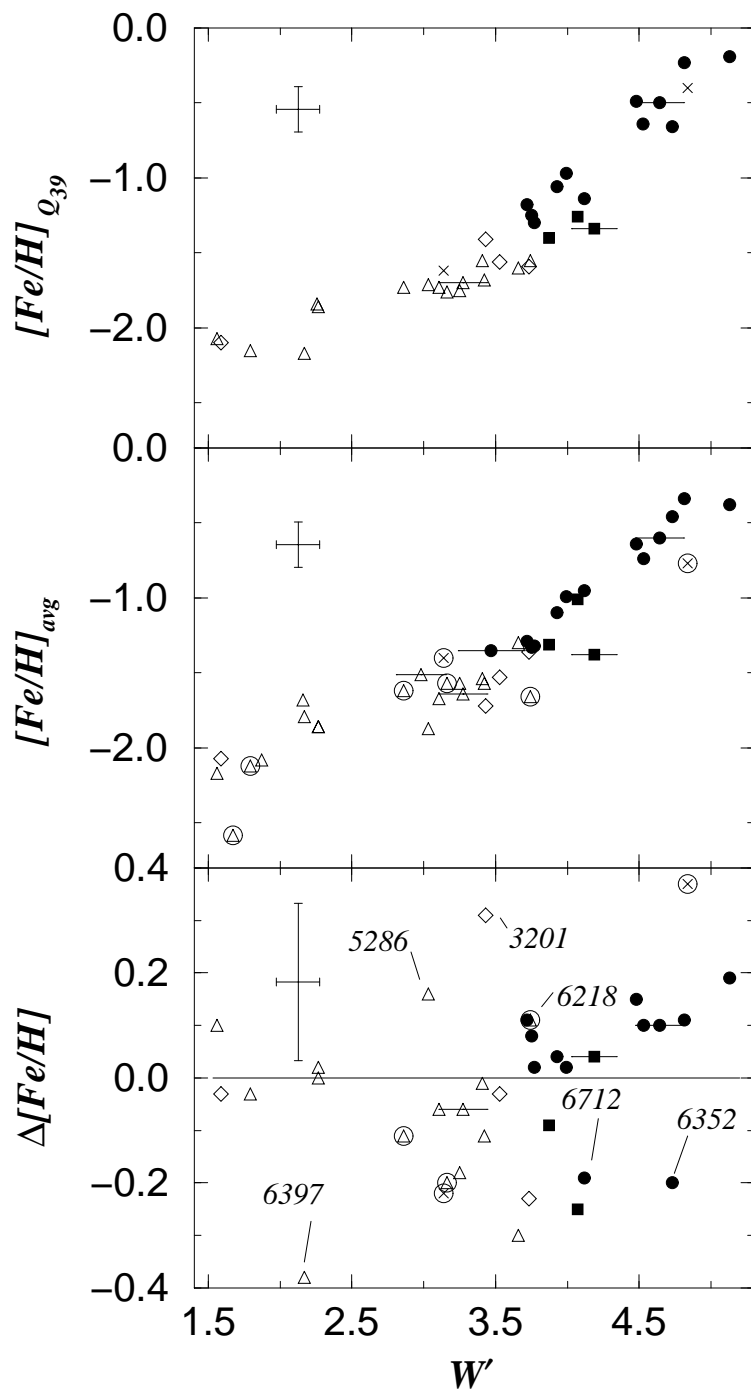


TABLE 3. [Fe/H] Values from High Dispersion Spectroscopy

NGC	Name	Cohen	GO89	M93	SKPL	BW	CG97
104	47 Tuc	-0.70	-0.82	...	...	-0.81	-0.70
288		-1.20	-1.31	...	...	...	-1.07
362		-1.25	-1.18	...	...	...	-1.15
1904		...	-1.42	...	...	...	-1.37
2298		...	...	...	...	...	-1.74
3201		-1.40	-1.34	...	...	...	-1.23
4590	M 68	...	-1.92	-2.17	...	...	-1.99
4833		...	-1.74	-1.71	...	...	-1.58
5897		...	-1.84	...	...	...	-1.59
5904	M 5	-1.45	-1.42	...	-1.17	...	-1.11
5927		-0.10	...	...	...	...	...
6121	M 4	...	-1.32	...	...	-1.21	-1.19
6144		...	...	-1.59	...	...	-1.49
6171	M 107	-0.90	...	...	...	...	...
6205	M 13	-1.60	...	...	-1.51	-1.87	-1.39
6254	M 10	...	-1.42	...	-1.52	...	-1.41
6352		-0.30	-0.79	...	...	...	-0.64
6362		...	-1.04	...	...	...	-0.96
6397		...	-1.88	-1.99	...	...	-1.82
6637	M 69	-0.85	...	...	...	...	...
6752		...	-1.53	-1.57	...	...	-1.42
6809	M 55	...	...	-1.95	...	...	...
6838	M 71	-0.75	-0.81	...	-0.79	...	-0.70
7078	M 15	-2.20	...	-2.23	-2.30	...	-2.12
7099	M 30	...	...	-2.11	...	...	-1.91
	Pal 12	...	...	...	...	-1.00	...

Notes to Table 3.

References— Cohen: Compilation in Frogel et al. (1983); GO89: Gratton and Ortolani (1989), and references therein; M93: Minniti et al. (1993); SKPL: Kraft et al. (1995), Sneden et al. (1994), Kraft et al. (1993), Sneden et al. (1992), Sneden et al. (1991); BW: Brown et al. (1996), Brown and Wallerstein (1992), Brown et al. (1991); CG97: Carretta and Gratton (1997).

Rutledge et al.: GGC CaII Metallicity Scale. II Analysis. -- Figure 4.

